INFACON 7, Trondheim, Norway, June 1995
Eds.: Tuset, Tveit and Page
Publishers: FFF, Trondheim, Norway

THERMAL BEHAVIOUR OF A SPHERICAL ADDITION TO MOLTEN METALS

Eirik Røhmen*, Trond Bergstrøm and Thorvald A. Engh***

* Faculty of Applied Earth Science and Metallurgy at the University of Trondheim
**Department of Materials Technology at the Foundation for Industrial and Technical Research at the Norwegian Institute of Technology.

ABSTRACT

The thermal behaviour of a spherical addition (granule) when added to a melt is studied. Additions with an exothermic heat of solution are not considered.

A general presentation of the mechanisms governing the dissolution of alloys in the cases where the dissolution rate is dominated by heat transfer from the melt to the alloy is given (when the addition melting point is lower than the bulk temperature). It can be shown that the rate of melting due to heat conduction would normally be at least 10 times faster than the dissolution governed by mass diffusion into the melt [1].

In order to study the formation and remelting of a layer of solidified melt (the shell) on the alloy addition during immersion, a series of experiments were performed on Al-spheres with diameter 50 mm. These experiments were performed with initial sphere temperature -196°C into water of 4°C and 18°C, and with initial sphere temperature 25°C into molten Al of temperature 720°C. The development of the shell and the temperatures at the sphere centre and surface was recorded. The results were compared with numerical calculations.

INTRODUCTION

Customer requirements are constantly increasing concerning composition and impurity limits for special purpose steels. This makes it ever more important to achieve exact knowledge of what happens during alloying, and what the effects are concerning alloying time, yield and impurity content.

For some additions, for instance FeSi and SiMn, melting times are long compared to the residence time in the bulk melt [2]. Typically, for 75% FeSi the residence time is less than half a second, while dissolution times vary from 1-2 seconds for 8 mm granules and up to 10 seconds for a 20 mm granule (the superheat was about 60°C). Clearly, these numbers tell us that the FeSi granule will rise to the top of the melt before it is fully melted. Since FeSi

is more reactive towards oxygen than iron [2], the result is often a reduced recovery of the alloy. It is therefore of interest to find wether the process parameters can be altered to achieve subsurface melting.

Questions of this kind concerning the dissolution of alloys, can often only be satisfactory answered if we know the exact kinetics involved. We must be able to determine quantities such as the heat transfer from the melt, the heat conduction inside the solid phases, the subsurface trajectory of the alloy etc. All these quantities depend on each other, and constitute a complex problem. In order to put reasonable limits on the problem, we have concentrated on the study of single spheres. We assume that the dissolution does not involve any exothermic reactions, that the melting is taken to be subsurface and that the heat transfer coefficient from the melt to the alloy is known. Within these limitations, we have developed a mathematical model that can predict dissolution times. In order to check the model, experiments have been performed on the freezing/melting of an ice layer on an immersed chilled aluminium sphere in water. Also the freezing/melting of an aluminum layer on aluminum spheres immersed in molten aluminium has been studied.

MATHEMATICAL TREATMENT OF THE MELTING OF A SINGLE SPHERE

The model presented here is made for calculating the melting time for alloys immersed into their own melt, or the shell period for alloys that has a higher melting point than the melt.

We assume that the heat transfer from the melt to the addition has spherical symmetry, and that the sphere is held motionless below the surface of the melt. The addition has an initial temperature T_0 and an initial radius r_0. The melt is assumed large enough to be treated as semi-infinite with temperature T_b. A shell of solidified melt will form around the addition when the initial temperature of the addition is below the melting point of the bulk material. After a while, the addition is sufficiently heated to allow this on-frozen bulk material to remelt. Thus the radius of the sphere will grow to a maximum at time t_m and then start to decrease until the shell is completely remelted at time t_s. This shell behaviour has been experimentally verified [3-5]. The shell is composed of the solidified melt and may of course have other physical properties than the addition.

The governing equations for the shell period are (for explanation of symbols, see nomenclature list at the end of the article):

alloy sphere: $0 \le r \le R_0$ and $0 \le t \le t_s$

$$\rho_a C_{pa} \frac{\partial T}{\partial t} = \frac{1}{r^2} \frac{\partial}{\partial r}\left[r^2 k_a \frac{\partial T}{\partial r} \right] \qquad (1)$$

shell: $R_0 < r \le R(t)$ and $0 \le t \le t_s$

$$\rho_s C_{ps} \frac{\partial T}{\partial t} = \frac{1}{r^2} \frac{\partial}{\partial r}\left[r^2 k_s \frac{\partial T}{\partial r} \right] \qquad (2)$$

With initial conditions

IC 1 $T = T_0$ $0 \le r \le R_0$ and for $t = 0$

IC 2 $R(t) = R_0$ for $t = 0$

The boundary conditions are listed from the sphere centre proceeding radially outward to the solid-melt interface.

BC 1 $\frac{\partial T}{\partial r} = 0$ $r = 0$ and for $0 \le t \le t_{total}$

BC 2 $\lim_{r \to R_0^-} T = \lim_{r \to R_0^+} T$ for $r = R_0$ and $t < t_s$

BC 3 $k_a \frac{\partial T}{\partial r} = k_s \frac{\partial T}{\partial r}$ for $r = R_0$ and $t < t_s$

BC 4 $T = T_{ms}$ for $r = R(t)$ and $t < t_s$

BC 5A $k_s \frac{\partial T}{\partial r} = [\rho_s \Delta H_{ms} + \rho_m C_{pm}(T_b - T_{ms})] \frac{dR}{dt} + h(T_b - T_{ms})$ for $r = R(t)$ and $t < t_m$

BC 5B $k_s \frac{\partial T}{\partial r} = \rho_s \Delta H_{ms} \frac{dR}{dt} + h(T_b - T_{ms})$ for $r = R(t)$ and $t_m < t < t_s$

If the addition is immersed into its own melt, it will start to melt when the shell has vanished. The heat conduction inside the sphere is still governed by Equation (1) but now with boundary conditions 1, 6 and 7:

BC 6 $T = T_{ma}$ for $r = R(t)$ and $t > t_s$

BC 7 $k_a \frac{\partial T}{\partial r} = \rho_a \Delta H_{ma} \frac{dR}{dt} + h(T_b - T_{ma})$ for $r = R(t)$ and $t > t_s$

Equations (1) and (2) are the heat diffusion equations in spherical coordinates. The first boundary condition expresses the spherical symmetry of the heat flow. This condition is valid until the alloy is completely melted. At times less than t_s, we have two boundary conditions on the sphere-shell interface. The first (BC 2) tells that there is no temperature gap, that is we assume that there is no thermal resistance across the interface. We also require that the heat flux leaving the shell must equal the heat flux entering the sphere (BC 3). These boundary conditions link the two heat equations together. On the shell-melt interface we demand that the shell surface temperature is constant and equal to the melting point of the bulk liquid. Boundary condition 5A is a heat balance for the moving shell solidification front when the front is advancing, ie. the shell is growing. This balance states that the heat entering the solid shell must equal the heat delivered from the melt by convective heat transfer and the heat delivered from solidification of melt plus the heat released by cooling the mass of

melt that solidifies from the bulk temperature T_b to the interface temperature T_{ms}. We must include this term when the interface is moving outwards since the heats released from both processes go from a higher to a lower temperature, and are therefore conducted into the solid phase. For some reason this sensible heat term is not given in the literature, possibly because it has been considered to be negligible. However, for instance for an aluminium melt with 60°C superheat, the term has a magnitude of 15% of the heat of fusion term, and is not negligible.

When the shell has started to melt, the situation is somewhat different. Then the heat balance reduces to (BC 5B): Heat delivered from the melt by convective conduction equals heat entering and heat used to melt the shell. The sensible heat term is not included since we assume that the melted shell mass is transported away by the bulk flow in the melt. Then the heating of the melted shell from temperature T_{ms} to T_b takes place at a position removed from the sphere surface. Thus we see that the heat balance is asymmetric with respect to the interface motion.

At times larger than t_s, the boundary conditions on the addition-melt interface are in principal the same as the shell-melt boundaries, except that the physical properties of the solid phase are linked to the alloy addition instead of to the shell. Then the surface temperature is set to the alloy melting point (BC 6), and the heat balance is given by boundary condition 7.

The heat transfer from the melt is dependent on the radius of the shell/addition. This dependency can be seen from a typical Nusselt number relation where $Nu = hd/k \sim Re^{1/2}$ which gives that the heat transfer coefficient goes like $h \sim d^{-1/2}$. This is taken care of by adjusting the heat transfer coefficient by the formula $h = h_0(d_0/d)^{1/2}$.

Apart from taking into account the sensible heat term and allowing the thermo-physical properties to vary with temperature the model is standard [4-7]. However, it will be seen that it is necessary to include a heat transfer resistance across the addition-shell interface. This will be treated in the discussion.

NUMERICAL CALCULATIONS

There exist no known analytical solutions to the mathematical model [8], and we must therefore solve the model numerically. We have written a computer program that can run on a conventional PC. In the program, we solve the heat diffusion equation with a partial implicit scheme developed by Patankar and Baliga [9]. This scheme which is a finite-difference scheme developed for parabolic differential equations, uses a power-law approximation which they claim possesses the accuracy of the Crank-Nicholson method and the physical realism of the fully implicit method. The Patankar and Baliga scheme is developed for stationary boundaries, ie. boundaries lying on a grid point. In order to handle the movement of the solid-melt interface which generally has positions between two grid points, we have modified a method given by Crank [10]. This is a front tracking method designed to work on a fixed finite difference grid.

As a check on the performance of the program, we calculated the shell formation on a cold sphere immersed in it's own melt with a temperature exactly at the melting point. Now, since the superheat is zero, the heat necessary to bring the sphere up to the melt temperature must come from solidification. For this case the shell thickness can also be found thermo-

dynamically: Then, if we disregard the temperature dependence of the physical properties, the heat balance becomes:

$$\frac{4}{3}\pi r^3 \rho_a \Delta H = \frac{4}{3}\pi[(r+\Delta r)^3 - r^3]\rho_a \Delta H_{ma} \quad (3)$$

ΔH is the difference in enthalpy for the sphere between room temperature and the melting point. Δr is the increment in the sphere radius, or the shell thickness which from Equation (3) is given as:

$$\Delta r = r[(\frac{\Delta H}{\Delta H_{ma}} + 1)^{\frac{1}{3}} - 1] \quad (4)$$

If we run the program with constant physical properties and set the bulk temperature equal to T_{ms}, it should give the same shell thickness as Equation (4). The result showed a discrepancy less than 1%.

EXPERIMENTAL PROCEDURE

In order to verify our model, we performed experiments on the shell formation on cold aluminium spheres immersed in water and on aluminium spheres immersed in molten aluminium. The water experiments include five series in water at 3.8°C and six series at 18.1°C. Each series involved 16 to 20 runs, and each run was performed with the same water and initial sphere temperature, convective conditions and sphere position in the water bath, but with different immersion times. The shell formation was measured by melting and weighing the on-frozen ice layer. In the 3.8°C experiments, the temperature at the sphere centre and surface was measured during the immersion. In order to eliminate any thermal

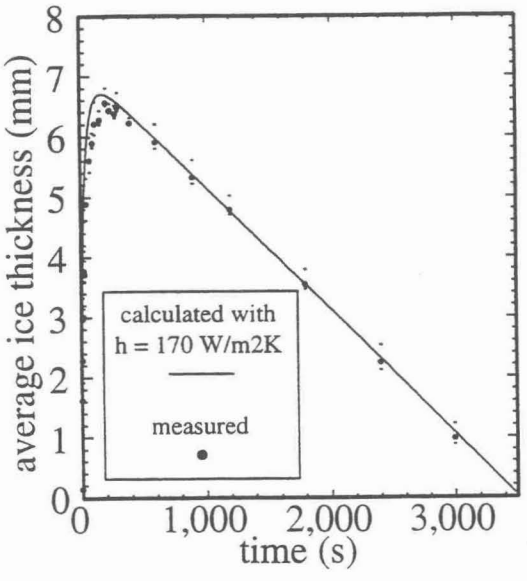

Figure 1 Calculated shell formation on a 4.85 cm diameter aluminium sphere chilled in liquid nitrogen and then immersed in water at 3.8°C. The heat transfer coefficient is fitted to give the measured slope of the shell melting rate.

Table 1 Data used in the calculation of the 3.8°C water experiments [11].

Data	
Sphere diameter (m)	0.0483
Initial sphere temperature, T_0 (K)	87.15
Melting point of aluminium, T_{ma} (K)	933.52
Melting point of ice, T_{ms} (K)	273.15
Bulk water temperature, T_b (K)	276.95
Heat of fusion of water (J/kg)	333548
Heat transfer coefficient (W/m^2K)	170
Density of water at temperature T_{ms} (kg/m^3)	999.8
Specific heat capacity of water at T_{ms} (J/kgK)	4217.7
Thermal conductivity of water at T_{ms} (W/mK)	0.5610

convection streams in the water bath, the experiments were performed in a refrigerated room so that the water had the same temperature as its surroundings.

The aluminium experiments consisted of four series with spheres at room temperature immersed in molten aluminium at 720°C. In each series 6 runs were made with presumed equal conditions but with different immersion time. The spheres were taken out of the bath after reaching the specified immersion time and the mass of the on-frozen shell was determined. The temperature was measured on the sphere surface and centre in each run. We attempted to have equal convective conditions in the melt by heating it to 20°C above the immersion temperature and then turning off the furnace power supply. The sphere was immersed when the melt had cooled to 720°C.

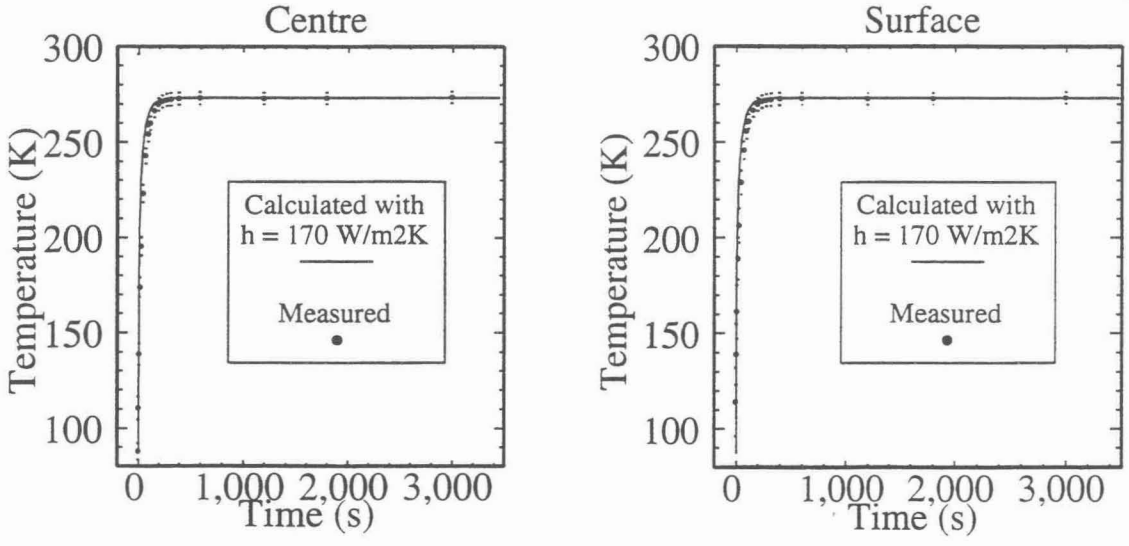

Figure 2 Calculated temperature profiles at the surface and centre of a 4.85 cm diameter aluminium sphere chilled in liquid nitrogen and then immersed in water at 3.8°C.

EXPERIMENTAL RESULTS AND DISCUSSION

Shell formation in the 4°C water experiments is presented in Figure 1 together with the calculated values. The calculations were performed taking into account the temperature dependence on the aluminum and ice density, thermal conductivity and specific heat capacity. The physical values employed are given in Table 1 and 2. The heat transfer coefficient was fitted from the slope of the ice melting rate at the end of the immersion period. We used the end of the period since then the sensible heat in the sphere has vanished, and all heat transferred from the melt is used to melt ice. Then the ice melting rate is completely determined by the heat transfer from the melt.

The measured and calculated temperature development at the sphere surface and centre in the 3.8°C experiments are given in Figure 2. From the figures we see that the calculated shell growth and temperature development in the 3.8°C experiments are in good agreement with the measured values. The calculated shell and temperature curves are a little to steep at the beginning of the immersion period. In the 18.1°C experiments an important effect emerges. In Figure 3 we show the measured and calculated shell formation, and from the figure we see that the calculated shell formation is over-estimated by more than 50%. This over-estimation becomes even more visible in a comparison of the calculated and measured shell formation

Table 2 Temperature dependent physical parameters used in the 3.8°C calculations [11-13].

Temperature (K)	ρ (kg/m^3)	C_p (J/kgk)	k (W/Mk)	Material
80.15	2734	357	380	
90.15	2733	422	-	
100.15	2732	482	300	
150.15	2726	289	247	
200.15	2719	791	237	Al
250.15	-	-	235	
273.15	-	-	236	
298.15	2701	897	-	
93.15	934	832.6	7.2	
123.15	933	1029.3	5.7	
153.15	931	1236.4	4.6	
173.15	929	1376.5	4.0	Ice
193.15	927	1508.3	3.5	
213.15	925	1640.1	3.0	
233.15	923	1804.4	2.7	
253.15	920	1959.4	2.4	
273.15	917	2116.9	2.3	

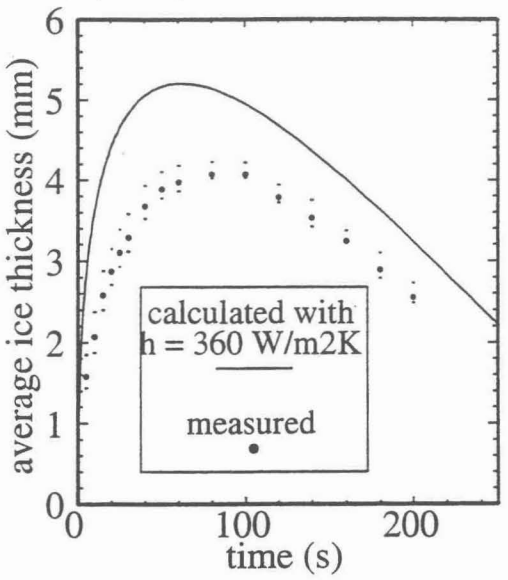

Figure 3 Calculated ice formation on a 4.85 cm diameter aluminium sphere chilled in liquid nitrogen and then immersed in water at 18.1°C. The heat transfer coefficient is fitted to give the measured slope of the shell melting rate.

in the aluminium experiments [1]. Then the shell over-estimation is more than 200%, and the calculated temperatures are also much higher than measured (the calculated centre temperature after being immersed for three seconds is more than 350°C higher than the measured temperature). It is also apparent from the figures that the calculated shell formation not only tends to be too large, but the maximum shell size tends to appear too early.

This over-estimation is taken as proof that there is a thermal resistance across the alloy-shell interface. In our model we assumed that the temperature on both sides of the interface is equal (BC 2). This means that there is perfect thermal contact between the addition and the on-frozen shell, i.e. there is no thermal resistance across the boundary. The heat transferred from the melt by convective conduction (the $h\Delta T$ term in BC 5A) is constant and independent of the conditions at the interface. Thus, if the heat flow across the interface is predicted to be too large, the shell will grow both faster and become thicker than measured because the alloy addition heat demand that exceeds the heat delivered from the melt is taken from solidification. Maximum shell thickness will also occur earlier since the larger the heat flow is across the interface, the faster the sphere acquires its sensible heat. At this point, the heat delivered by the melt will dominate and the shell will remelt. The over-estimation was only barely present in the early shell period in the 3.8°C water experiments; it became more visible in the 18.1°C experiments and totally dominant in the aluminium series. This fact also supports the presence of an inner heat transfer resistance, since this effect should only be visible before the sphere temperature approaches the melting point. Thus the smaller time scale and the larger the heat flows are, the more visible should the disregard of heat transfer resistance across the interface be. And this is what we observe.

We assume that the thermal resistance is due to a thin layer with thickness δ that separates the sphere and shell, and that the temperature profile in the layer is a straight line. Then the

Table 3 Data used in the calculation of the aluminium spheres immersed in molten aluminium at 720 °C [11, 12 and 14].

Data	
Sphere diameter (m)	0.049
Initial sphere temperature, T_0 (K)	298.15
Melting point of aluminium, T_{ma} (K)	933.52
Bulk temperature, T_b (K)	993.15
Heat of fusion of aluminium (J/kg)	396998
Heat transfer coefficient (W/m^2K)	14500
Melt density at temperature T_b (kg/m^3)	2367.1
Specific heat capacity of the melt at T_b (J/kgk)	1176.8
Thermal conductivity of the melt at T_b (W/Mk)	92.8

heat flux across the layer is given as $\dot{q} = h_\delta(T_{si} - T_{ai})$ where T_{si} is the temperature on the inner surface of the shell and T_{ai} is the temperature on the sphere surface. We have assumed then that the layer is so thin that its thermal capacity is negligible. Also it does not give a noticeable contribution to the radius of the system. Then we can employ our existing model

Table 4 Input of the temperature dependent physical parameters used in the calculation of the melting of the aluminium sphere immersed in molten aluminium at 720 °C [11, 12, 14 and 15].

Temperature (K)	Al		
	ρ (kg/m^3)	C_p (J/kgk)	k (W/Mk)
273.0	2706	870.1	236
298.15	2701	897.2	236.9
300.0	2701	898.7	237
350.0	2691	927.1	240
400.0	2680	955.6	240
500.0	2661	994.8	237
600.0	2639	1033.5	232
700.0	2615	1078.5	226
800.0	2591	1132.7	220
900.0	2567	1197.4	213
933.33	2559	1221.5	210

if we substitute boundary condition 2 with:

BC 2A $\lim_{r \to R_0^-} T = T_{ai}$ *and* $\lim_{r \to R_0^+} T = T_{si}$ for r = R_0 and t < t_s

and boundary condition 3 with:

BC 3A $$k_a \frac{\partial T}{\partial r} = k_s \frac{\partial T}{\partial r} = h_\delta (T_{si} - T_{ai})$$ for r = R_0 and t < t_s

We used the measured shell thickness and temperature at the sphere surface to fit both the inner and outer heat transfer coefficients. In Figure 4 we show the calculated and measured shell growth, and the temperature at the sphere surface for the aluminium experiments. The calculations were performed with the physical constants given in Tables 3 and 4.

One fortunate and interesting property of the temperature development inside the sphere is that it is practically independent of the outer heat transfer coefficient. This can be demonstrated by calculating the temperature at the sphere surface with different values of the outer heat transfer coefficient h. We have performed these calculations using the original numerical model, in order to avoid confusion with the effect of the inner heat transfer resistance. The resulting surface temperature developments from the four calculations are nearly identical as shown in Figure 5. The surface temperatures differs by less than one percent after 12 seconds immersion. This means that the rate at which the addition is heated is independent of the heat transfer conditions in the melt. This implies that, no matter how much stirring or superheat is employed, the time needed to bring the alloy up to its melting point is practically the same. If there is an internal heat transfer resistance, the heat rate is

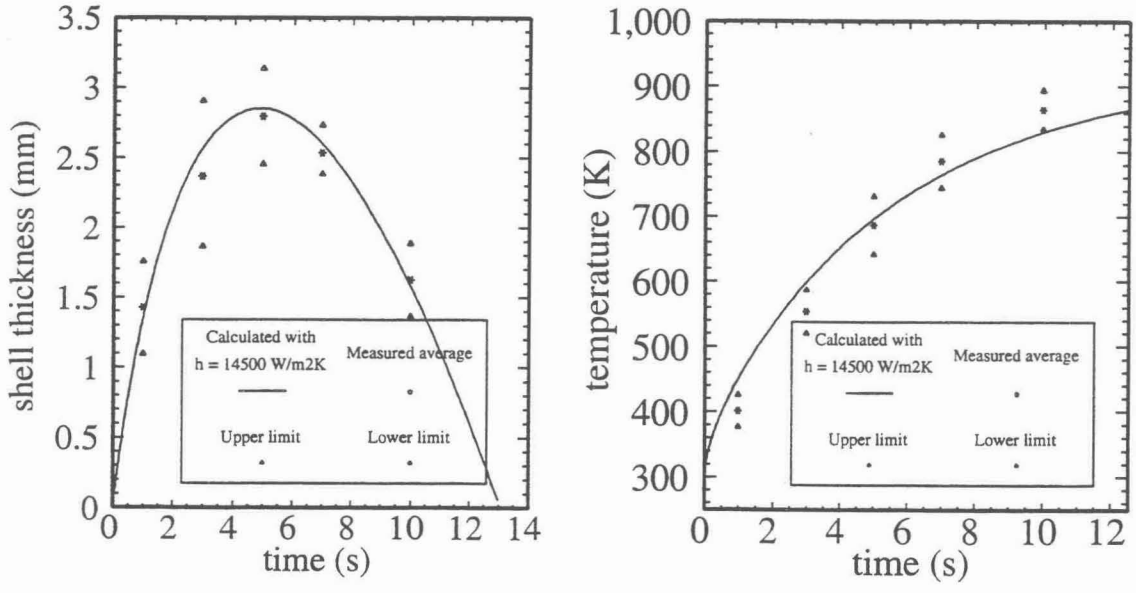

Figure 4 Calculated and measured shell formation and surface temperature on a 4.9 cm diameter aluminium sphere immersed in molten aluminium at 720°C. In the calculations we assumed a constant thermal resistance across the addition-shell interface. Both the inner and outer (shell-melt) heat transfer coefficients are fitted by the slope of the calculated shell curve. h_δ = 4000 W/m^{2}K.

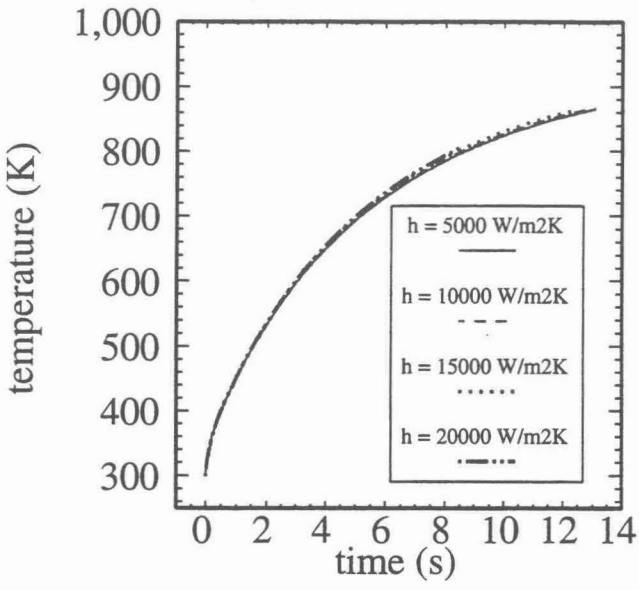

Figure 5 Calculated temperature at the centre of an 4.9 cm aluminium sphere immersed in molten aluminium at 720°C for four different values of the outer heat transfer coefficient.

determined by the alloy addition transport properties and the thermal contact between the alloy and shell. In order to check that this effect is not accidental, similar calculations have been performed on FeSi granules [1].

The result given above is especially important for alloys that react strongly exothermically with liquid steel such as FeSi and SiMn. Argyropoulos and Guthrie [3] have shown that the exothermic reaction between a 50wt% ferro-silicon alloy and its on-frozen steel shell is ignited when the alloy-shell interface reaches 1260°C. The reaction is both violent and rapid and one may in practice consider the alloy to be melted as soon as the "ignition" temperature is reached. Since addition temperature hardly depends on heat transfer from the melt, the time taken to achieve ignition temperature is independent of melt stirring. Due to the importance of the inner heat transfer coefficient, serious consideration should be given to enhance the thermal contact between the alloy addition and its on-frozen shell.

CONCLUSIONS

1 A comprehensive mathematical/numerical model is developed for calculating the dissolution times for spherical alloy additions to liquid metals. Temperature profiles and heat flows are assumed to be spherically symmetric.

2 The rate at which the alloy addition is heated during the shell period, is completely determined by the thermal transport properties of the addition and the thermal contact between the addition and it's on-frozen shell. The heat transfer from the melt is of little importance for the temperature profile in the addition.

3 For alloy additions that react strongly exothermically with the melt, the thermal properties of the addition and the inner heat resistance determines the rate at which the alloy dissolves.

4 To give satisfactory comparison between experimental and numerical results an initial heat transfer resistance between the addition and the on-frozen shell has to be included in the computations.

5 Ideally, this model should be used in conjunction with calculations of residence times and sub-surface trajectories.

ACKNOWLEDGEMENTS

The authors wish to thank the Norwegian Research Council and The Ferroalloy Research Association for financial support that made this work possible.

NOMENCLATURE

C_{pa}	Specific heat capacity of the addition (J/kgk).
C_{pm}	Specific heat capacity of the liquid melt (J/kgk).
C_{ps}	Specific heat capacity of the shell (J/kgk).
d	Diameter (m).
d_0	Initial diameter of the addition (m).
h	Heat transfer coefficient for the heat flow across the shell-melt interface (W/m^2K).
h_δ	Heat transfer coefficient for the heat flow across the addition-shell interface (W/m^2K).
ΔH	Enthalpy (J/kg).
ΔH_{ma}	Heat of fusion for the addition (J/kg).
ΔH_{ms}	Heat of fusion for the shell (J/kg).
k_a	Thermal conductivity of the addition (W/Mk).
k_s	Thermal conductivity of the shell (W/Mk).
r	Radial coordinate (m).
Δr	Increase in addition radius (shell thickness) (m).
R_0	Initial radius of the addition.
$R(t)$	Radius at time t (m).
t	Time coordinate (s).
t_m	Time when the shell reaches maximum thickness (s).
t_s	Shell lifetime (s).
t_{total}	Dissolution time (s).
T	Temperature coordinate (K).
T_{ai}	Temperature at the addition surface (K).
T_b	Bulk temperature of melt (K).
T_{ma}	Melting point of the addition (K).
T_{ms}	Melting point of the shell (K).
T_0	Initial temperature of addition (K).
T_{si}	Temperature at the inner surface of the shell (K).
δ	Layer thickness (m).
ρ_a	Density of the addition (kg/m^3).
ρ_m	Density of the liquid melt (kg/m^3).
ρ_s	Density of the shell (kg/m^3).

REFERENCES

1. Røhmen E., Dr.ing. thesis at NTH, University of Trondheim. To be published in march 1995.
2. Lee Y. E., Tveit H. and Guthrie R.I.L., "Model study for subsurface trajectory of 75FeSi and SiMn ferroalloys in steel", *Steel Research*, vol. 9, 1992, pp. 379-386.
3. Argyropoulos S. A. and Guthrie R.I.L., "The Exothermic Dissolution of 50wt% Ferro-Silicon in Molten Steel", *Canadian Metallurgical Quarterly*, vol. 18, 1979, pp. 267-281.
4. Ehrich O., Chuang Y. K. and Schwerdtfeger K, "The melting of sponge iron spheres in their own melt", *Arch. Eisenhüttenwesen*, vol. 50, 1979, pp. 329-334.

5. Taniguchi S., Ohmi M. and Ishiura S., " A Hot Model Study on the Effect of Gas Injection upon the Melting Rate of Solid Sphere in a Liquid Bath", *Transactions ISIJ*, vol. 23, 1983, pp. 571-577.
6. Szekely J., Chuang Y. K. and Hlinka J. W., "The Melting and Dissolution of Low-Carbon Steels in Iron-Carbon Melts", *Metallurgical Transactions*, vol. 3, 1972, pp. 2825-2833.
7. Seaton C. E., Rodríguez A. A., González M. and Manrique M., "The Rate of Dissolution of Pre-reduced Iron in Molten Steel", vol. 23, 1983, pp. 14-20.
8. Alexiades V. and Solomon A. D., "Mathematical Modelling of Melting and Freezing Processes", Hemisphere Publishing Corporation, Washington, 1993.
9. Patankar S. V. and Baliga B. R., "A New Finite-Difference Scheme for Parabolic Differential Equations", *Numerical Heat Transfer*, vol. 1, 1978, pp. 27-37.
10. Crank J., "Free and Moving Boundary Problems", Clarendon Press, Oxford, 1984.
11. Weast R.C., Editor, "CRC Handbook of Chemistry and Physics", 60th Edition, 1980, CRC PRESS Inc.
12. Perry R. H. and Green D. W., Editors, "Perry's Chemical Engineers Handbook", Sixth Edition, 1984, McGraw-Hill Book Company.
13. Landolt and Börnstein, Editors, "Zahlenwerte und Funktionen aus Physik, Chemie, Astronomie, Geophysic und Technik", vol. 4 Wärmetechnik, p. 517, Springer Verlag, Berlin.
14. Chase M. W. et al, Editors, "JANAF Thermochemical Tables Third Edition", *J. Phys. Chem. Ref. Data*, vol. 14, Suppl. 1.
15. Engh T. A., "Principles of Metal Refining", Oxford University Press, 1992.